

Style and Pose Control for Image Synthesis of Humans from a Single Monocular View

KRIPASINDHU SARKAR, Max Planck Institute for Informatics
 VLADISLAV GOLYANIK, Max Planck Institute for Informatics
 LINGJIE LIU, Max Planck Institute for Informatics
 CHRISTIAN THEOBALT, Max Planck Institute for Informatics

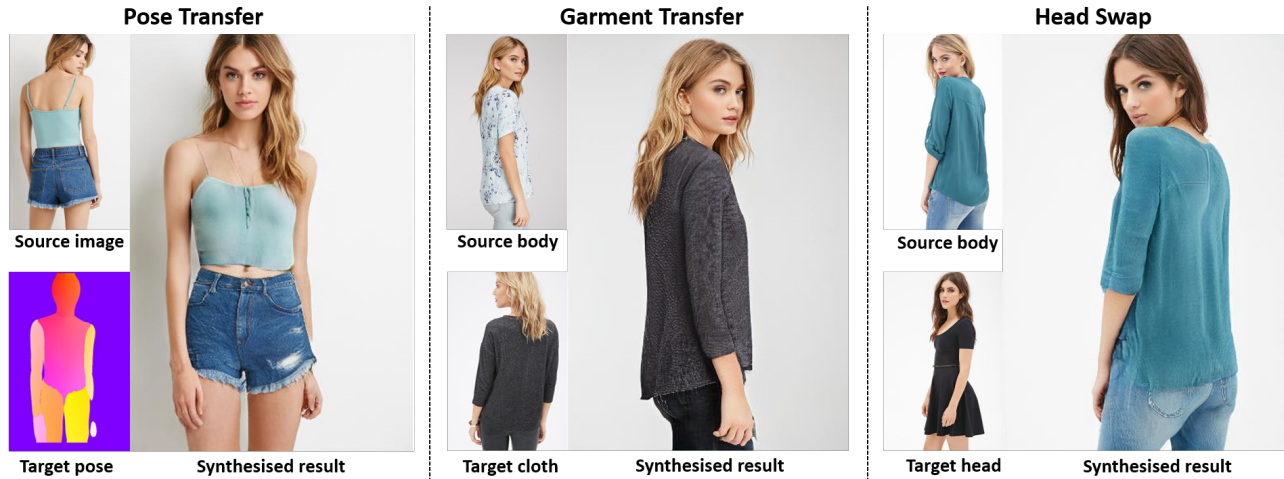


Fig. 1. We present StylePoseGAN, *i.e.*, a new approach for synthesising photo-realistic novel views of a human from a single input image with explicit control over pose and per-body-part appearance. We generate images of higher fidelity compared to the state-of-the-art methods, especially with fine appearance details such as faces and texture patterns. Our method enables several applications such as pose transfer, garment transfer, and head swap. All synthesised results in this figure are shown as obtained from our model without further post-processing.

Photo-realistic re-rendering of a human from a single image with explicit control over body pose, shape and appearance enables a wide range of applications, such as human appearance transfer, virtual try-on, motion imitation, and novel view synthesis. While significant progress has been made in this direction using learning-based image generation tools, such as GANs, existing approaches yield noticeable artefacts such as blurring of fine details, unrealistic distortions of the body parts and garments as well as severe changes of the textures. We, therefore, propose a new method for synthesising photo-realistic human images with explicit control over pose and part-based appearance, *i.e.*, StylePoseGAN, where we extend a non-controllable generator to accept conditioning of pose and appearance separately. Our network can be trained in a fully supervised way with human images to disentangle pose, appearance and body parts, and it significantly outperforms existing single image re-rendering methods. Our disentangled representation opens up further applications such as garment transfer, motion transfer, virtual try-on, head (identity) swap and appearance interpolation. StylePoseGAN achieves state-of-the-art image generation fidelity on common perceptual metrics compared to the current best-performing methods and convinces in a comprehensive user study.

Authors' addresses: KRIPASINDHU SARKAR, Max Planck Institute for Informatics, ksarkar@mpi-inf.mpg.de; VLADISLAV GOLYANIK, Max Planck Institute for Informatics, golyanik@mpi-inf.mpg.de; LINGJIE LIU, Max Planck Institute for Informatics, lliu@mpi-inf.mpg.de; CHRISTIAN THEOBALT, Max Planck Institute for Informatics, theobalt@mpi-inf.mpg.de.

Additional Key Words and Phrases: Pose Transfer, StylePoseGAN, Garment Transfer, Identity Swap

1 INTRODUCTION

Creating photo-realistic images and videos of humans under full control of pose, shape and appearance is a core challenge in computer animation with many applications in movie production, content creation, visual effects and virtual reality, among others. Achieving this with the established computer graphics toolchains is an extremely complex and time-consuming process. First, a high-quality 3D human geometry and appearance model is required either manually designed by skilled artists or captured with dense camera arrays. To make the model animatable, sophisticated rigging techniques need to apply, and some manual post-processing (*e.g.*, skinning weight painting) is often required. After that, computationally-expensive global illumination rendering techniques are needed to render the model photo-realistically. Some works [Casas et al. 2014; Volino et al. 2014; Xu et al. 2011] attempted to avoid such sophisticated toolchains with image-based rendering (IBR) techniques. However, these methods still have sub-optimal rendering quality and limited control over the renderings and are often scene-specific.

Recently, great progress in learning-based approaches for image synthesis from a single monocular input view has been made



Fig. 2. Most of the recent human re-rendering methods cannot recover the fine texture details. Here we show the result of the recent state-of-the-art method of NHRR [Sarkar et al. 2020] and compare it with ours.

[Alldieck et al. 2019; Esser et al. 2018; Grigor’ev et al. 2019; Kratzwald et al. 2017; Lazova et al. 2019; Neverova et al. 2018; Pumarola et al. 2018; Sarkar et al. 2020; Siarohin et al. 2018; Yoon et al. 2020]. However, because of the underconstrained nature of this problem, most methods have limits in the visual quality of the results. They frequently exhibit oversmoothing, add unrealistic textures, lack fine-scaled details and wrinkle patterns, and lose facial identity.

This paper proposes a new lightweight learning-based approach for photo-realistic controllable human image generation, *i.e.*, StylePoseGAN, that enables fine-grained control over the generated human images and significantly outperforms all tested competing methods for re-rendering of humans from a single image, see Fig. 1 for the method overview. Our approach works with a single camera only, and no expensive set-ups and manual user interaction are required. At its core is a conditional generative model with several lightweight proxies, enabling control over body pose and appearance from a single image.

Our approach is an extension of non-controllable¹ and the state-of-the-art photo-realistic generative models for human portraits such as StyleGAN [Karras et al. 2019, 2020]. StylePoseGAN improves upon it by conditioning pose as spatial features and conditioning appearance for the weight demodulation. Our model can be trained in a fully supervised way with human images that enables the reconstruction of images with a forward pass. Such an approach results in significantly fewer artefacts and better preservation of fine texture patterns, compared to the results of existing methods (Sec. 4). Due to the separate conditioning of two aspects in different modalities, our design explicitly disentangles pose, appearance and body parts, and opens up several applications such as pose transfer, garment transfer, motion transfer and parts-swap. Compared to state of the art, we support much finer texture details and richer texture patterns of the garments, which is one of the strongest properties of StylePoseGAN, see Fig. 2 for qualitative comparison with NHRR [Sarkar et al. 2020]. To summarise, our technical **contributions** are:

- StylePoseGAN, *i.e.*, a disentangled architecture for human image generation which pushes the attainable visual quality of the generated human images significantly.
- State-of-the-art results on the DeepFashion dataset [Liu et al. 2016] which are confirmed with quantitative metrics, and qualitatively with a user study.

¹not controllable for style and pose on the level of traditional graphics pipelines

- Support of richer texture and pose-dependent effects such as wrinkles and shadings, compared to the current state of the art.
- Applications of StylePoseGAN in image manipulation, *i.e.*, garment transfer, head (identity swap) and image interpolation, which enable special effects which can be useful in computer animation.

We evaluate our method on several datasets and report perceptual metrics. Additionally, we conduct a comprehensive user study. We encourage the readers to watch our supplementary video.

2 RELATED WORK

We next review related works in human rendering, deep generative models and human pose transfer.

2.1 Classical and Neural Rendering of Humans

Photo-realistic rendering of a real human using classical rendering methods heavily relies on a high-quality geometry and appearance human model. To achieve high quality, real individuals need to be captured with sophisticated scanners and reconstructed by 3D reconstruction techniques. To synthesise the human image in a new pose, some sophisticated rigging techniques need to be applied to rig the human model, and a mapping from body poses to pose-dependent appearance or geometry models need to be learned. [Xu et al. 2011] propose a method which first retrieves the most similar poses and view-points in a pre-captured database and then applies retrieval-based texture synthesis. [Casas et al. 2014; Volino et al. 2014] compute a temporally coherent layered representation of appearance in texture space. However, the synthesis quality is limited by the quality of the geometry and appearance human model. To address the limitations of classical rendering methods, recent works integrated deep learning techniques into the classical rendering pipelines. Some methods [Kappel et al. 2020; Kim et al. 2018; Liu et al. 2020b, 2019; Meshry et al. 2019; Thies et al. 2019; Yoon et al. 2020] first render 2D/3D skeleton, 2D joint heat maps, or a coarse surface geometry with explicit or neural textures into coarse RGB images or feature maps which are then translated into high-quality images using image translation networks, such as pix2pix [Isola et al. 2017]. Another line of works learn scene representations for novel view synthesis from 2D images. Although this kind of methods achieves impressive renderings of static [Liu et al. 2020a; Mildenhall et al. 2020; Sitzmann et al. 2019a,b; Zhang et al. 2020] and dynamic scenes and enables playback and interpolation [Gafni et al. 2020; Li et al. 2020; Lombardi et al. 2019; Park et al. 2020a; Pumarola et al. 2020; Raj et al. 2020; Sida Peng 2020; Tretschk et al. 2020; Wang et al. 2020; Xian et al. 2020; Zhang et al. 2020], it is not straightforward to extend these methods to synthesise human images of the full body with explicit control. Moreover, most of them are scene-specific. In contrast, our StylePoseGAN builds upon deep generative models and can synthesise photo-realistic human images with explicit control over body pose and human appearance.

2.2 Deep Generative Models

Generative Adversarial Networks (GAN) have made remarkable achievements in image generation in recent years. A GAN model

has two components: generator and discriminator. The core idea of a GAN model is to use a generator to synthesise a candidate image from a noise vector z sampled from the distribution of training images and let the discriminator evaluate whether the candidate is real or fake. The two components are trained together until the image generated by the generator is realistic enough to fool the discriminator. The first GAN model was introduced by Goodfellow et al. [2014], which was only able to synthesise low-resolution images with limited quality. To improve the quality, SAGAN [Zhang et al. 2019] introduces a self-attention mechanism into convolutional GANs, which allows the generator synthesising details using cues from all feature locations and the discriminator checking features in global image space. BigGAN [Brock et al. 2018] makes multiple changes on SAGAN for quality improvement. ProGAN [Karras et al. 2018] demonstrates photo-realistic images of human faces in a high resolution of 1024×1024 by training the generator and discriminator progressively from low resolution to high resolution. Since these methods use a single latent vector z to resemble the latent distribution of training data, they cannot disentangle different attributes in the images so have limited control over image synthesis. StyleGANs [Karras et al. 2019, 2020] approach this problem by mapping z to an intermediate latent space w , which is then fed into the generator to control different levels of attributes. Although they provide more control on image synthesis, it is still not able to completely disentangle different semantically meaningful attributes and control them in the synthesis. Recent works [Tewari et al. 2020a,b] extend StyleGAN to synthesise face images with a rig-like control over 3D interpretable face parameters such as face pose, expressions and scene illumination. GAN-control [Shoshan et al. 2021] employ contrasting learning to train GANs with an explicitly disentangled latent space for faces, which can control identity, age, pose, expression, hair colour and illumination. Compared to faces, synthesising the full human appearance with control of 3D body pose and human appearance is a much more difficult problem due to more severe 3D pose and appearance changes.

Conditional GAN (cGAN) is a type of GAN, which provides conditional information for the generator and discriminator. cGAN is useful for applications such as class conditional image generation [Mirza and Osindero 2014; Miyato and Koyama 2018; Odena et al. 2017] and image to image translation [Isola et al. 2017; Wang et al. 2018b]. Most works [Isola et al. 2017; Mirza and Osindero 2014; Park et al. 2019; Wang et al. 2018a,b] require paired data for fully-supervised training. pix2pix [Isola et al. 2017] and pix2pixHD [Wang et al. 2018b] learn the mapping from input images to output images. GauGAN [Park et al. 2019] focuses on image generation from segmentation masks and designs an interactive tool for users to control over semantic and style in the image synthesis. To tackle the setting that paired data are unavailable, some works [Bansal et al. 2018; Choi et al. 2018; Liu et al. 2017a; Yi et al. 2017; Zhu et al. 2017] learn the mapping between two domains based on unpaired data. CycleGAN [Zhu et al. 2017] introduces a cycle consistency loss to enforce the translation property, *i.e.*, that the inverse mapping of a mapping of an image should result in the original image. We propose a method that extends StyleGANs [Karras et al. 2019, 2020] and can synthesise photo-realistic images of a full human body with explicit control over 3D poses and the appearance of

each body part. A concurrent work [Lewis et al. 2021] is similar to our method, which proposed a pose-conditioned StyleGAN2 latent space interpolation for virtual try-on. In contrast to their method, 1) we represent appearance in a pose independent normalised space which makes part based conditioning easier, 2) we use an explicit appearance encoder to encode the part based appearance latent vector z with a single forward pass instead of optimizing for z , 3) we do not use explicit supervision through segmentation masks as needed in [Lewis et al. 2021] for latent code optimisation.

2.3 Human Pose Transfer

The human pose transfer problem is defined as transferring person appearance from one pose to another [Ma et al. 2017]. Most approaches formulate it as an image-to-image mapping problem, *i.e.*, given a reference image of the target person, mapping the body pose in the format of renderings of a skeleton [Chan et al. 2019; Kratzwald et al. 2017; Pumarola et al. 2018; Siarohin et al. 2018; Zhu et al. 2019], dense mesh [Grigor’ev et al. 2019; Kappel et al. 2020; Liu et al. 2020b, 2019; Neverova et al. 2018; Sarkar et al. 2020; Wang et al. 2018a; Yoon et al. 2020] or joint position heatmaps [Aberman et al. 2019; Ma et al. 2017, 2018] to real images. Ma et al. [2017] design a two-stage framework, which first generates a coarse image of the person in the reference image with the target pose and refines the coarse image with a UNet trained in an adversarial way. To better preserve the appearance from the reference image to the generated image, some methods [Liu et al. 2020b; Sarkar et al. 2020] first map the human appearance in the screen space to UV space and feed the rendering of the person in the target pose with the UV texture map into an image-to-image translation network. Thanks to the explicit control over the pose and per-body-part appearance, StylePoseGAN can perform not only pose transfer but also be used for garment transfer and identity exchange.

3 METHOD

Given a single image I of a person, our goal is to synthesise a new image of the same person in a different target body pose. The overall idea can be summarised as follows. We first extract pose P and appearance A from I . Second, we encode pose and appearance to the tensor encoding E and z , respectively where E is a 3D tensor with spatial dimensions (height and width), whereas z is a vector. We then reconstruct I using a high-fidelity style-based generator with z as the noise vector and E as the spatial input. The pose and appearance are further disentangled by training with the source (s) – target (t) image pairs (I_s, I_t) of the same person with different poses, where we use the appearance of source A_s and the pose of the target P_t to reconstruct I_t in a fully supervised manner. Our method is summarised in Fig. 4, and is described in detail in the following.

3.1 Pose and Appearance Extraction

We use DensePose [Gueler et al. 2018] to detect the human pose $P \in \mathbb{R}^{H \times W \times 3}$ from the image I , and represent the appearance $A \in \mathbb{R}^{H_a \times W_a \times 3}$ with the partial texture map of the underlying SMPL mesh. Here, $H \times W$ is the resolution of the generated image (with H and W denoting its height and width, respectively), and $H_a \times W_a$

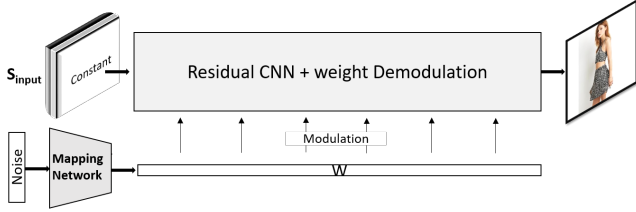


Fig. 3. **The original StyleGAN2 architecture** [Karras et al. 2020]. StyleGAN-based methods take a constant 3D tensor with spatial dimensions (with a predefined $height \times width \times channel$) as input which is translated to the three-channel output image by series of *demodulated* convolutions controlled by the learned latent vector W . In StylePoseGAN, we use the tensor S_{input} to provide spatial conditioning, while W is used for appearance conditioning. See Fig. 4 for an overview of our method and further details.

is the resolution of the texture image (with H_a and W_a denoting its height and width, respectively). DensePose provides pixelwise correspondences between a human image and the texture map of a parametric model of human SMPL [Loper et al. 2015]. This makes the computation of the partial texture from the visible body parts in the human image possible with a single sampling operation. The ResNet-101-based DensePose network provided by the authors is pre-trained on COCO-DensePose dataset, and outputs 24 part-specific U, V coordinates of the SMPL model. For easier mapping, the 24 part-specific UV-maps are combined to a single UV-texture map A in the format provided in the SURREAL dataset [Varol et al. 2017] through a pre-computed lookup table.

The normalised texture map provides a pose-independent appearance encoding of the subject, where each part (out of 24) is assigned a specific region or a set of pixels in A . Therefore, we can perform part-specific conditioning for the parts $p_i, i \in \{1, \dots, 24\}$ by changing values at its corresponding region $A[S_{p_i}]$. Here, $S_{p_i} \subset \mathbb{R}^{H_a \times W_a}$ are the pixel locations of the part p_i in the normalised texture map, and $A[\cdot]$ is the indexing operation. See Fig. 5, 6 and Sec. 3.6.2 for more details.

3.2 Pose and Appearance Encoding

PNet. We encode P by a fully convolutional network *PNet* comprising four downsampling residual blocks that produce the encoded pose $E \in \mathbb{R}^{H/16 \times W/16 \times 512}$. Note that based on the design of the generator that is used subsequently in our architecture, we do not need an explicit pose encoder. However, an encoded tensor with smaller spatial dimension is more suited for the StyleGAN2 based generator. See Secs. 3.3 and 4.3 for more details.

ANet. The appearance encoder *ANet* has the same architecture as *PNet* in its initial part. In contrast to *PNet*, its spatial activation volume is further passed through convolutional layers and, finally, a fully connected layer to produce the appearance encoding $z \in \mathbb{R}^{2048}$. Despite of the common architecture in the initial layers, *ANet* and *PNet* do not share any weights.

3.3 Image Generation with a Style-based Generator

We use a StyleGAN2-based generator [Karras et al. 2020] *GNet* that combines the pose encoding E and the appearance encoding z to

reconstruct back the input image $I = GNet(E, z)$. The original StyleGAN takes a constant tensor S_{input} with spatial dimensions (with a predefined $height \times width \times channel$) as input on which convolutions are performed. A separate latent noise vector that controls the generated image is passed through a mapping network, and its output w is used to modulate the weights of the convolution layers, see Fig. 3. We observe that the tensor S_{input} can be used to provide spatial condition to the generator, instead of keeping it constant. Therefore, our *GNet* takes E as input to the convolutional layers. The convolutional weights are demodulated using the encoded appearance z to finally reconstruct the image I . It comprises four residual blocks and four upsample residual blocks that transform an input tensor of dimensions $H/16 \times W/16 \times 512$ to an RGB image of dimensions $H \times W \times 3$. The architectural design of *GNet* follows StyleGAN2 [Karras et al. 2020] including bilinear upsampling, equalised learning rate, noise injection at every layer, adjusting variance of residual blocks and leaky ReLU. See Fig. 4 for an overview of StylePoseGAN.

3.4 Pose-Appearance Disentanglement by Paired Training

When the images of the same person in different poses are available for training, we can use them to further disentangle the pose and appearance. Given the source and target image pair (I_s, I_t) of the same subject, we extract the corresponding appearances and poses A_s, A_t, P_s and P_t . Next, we encode the poses and appearances using *P-Net* and *A-Net* to obtain the encodings E_s, E_t, z_s and z_t . Finally, we generate the images I'_s and $I'_{s \rightarrow t}$ as

$$\begin{aligned} I'_s &= GNet(E_s, z_s), \text{ and} \\ I'_{s \rightarrow t} &= GNet(E_s, z_t). \end{aligned} \quad (1)$$

Here $I'_{s \rightarrow t}$ is the generated image of the source appearance in the target pose, which can be directly supervised during the training.

3.5 Training Details and Loss Functions

Given the input pairs (I_s, I_t) and the generated images $I'_s, I'_{s \rightarrow t}$, the entire architecture is trained end-to-end for the parameters of *PNet*, *ANet* and *GNet*. We optimise the following loss:

$$\mathcal{L}_{total} = \mathcal{L}(I'_s, I_s) + \mathcal{L}(I'_{s \rightarrow t}, I_t) + \lambda_{patch} L_{patch}(I'_{s \rightarrow t}, I_t). \quad (2)$$

The total loss \mathcal{L}_{total} consists of reconstruction loss $\mathcal{L}(\cdot)$ and patch co-occurrence loss $L_{patch}(\cdot)$. The reconstruction loss

$$\mathcal{L}(I_{gen}, I_{gt}) = \lambda_{L1} L_1 + \lambda_{VGG} L_p + \lambda_{face} L_{face} + \lambda_{GAN} L_{GAN} \quad (3)$$

comprises the following terms:

- *L₁ reconstruction loss*. We use L_1 distance as a reconstruction loss to force I_{gen} and I_{gt} to be close to each other:

$$L_1 = |I_{gen} - I_{gt}|. \quad (4)$$

- *Perceptual Reconstruction Loss*. We use a perceptual loss [Johnson et al. 2016] based on the VGG Network to enforce perceptual similarity between generated and the ground truth image. It is defined as the difference between the activations on different layers of the pre-trained VGG network [Simonyan and

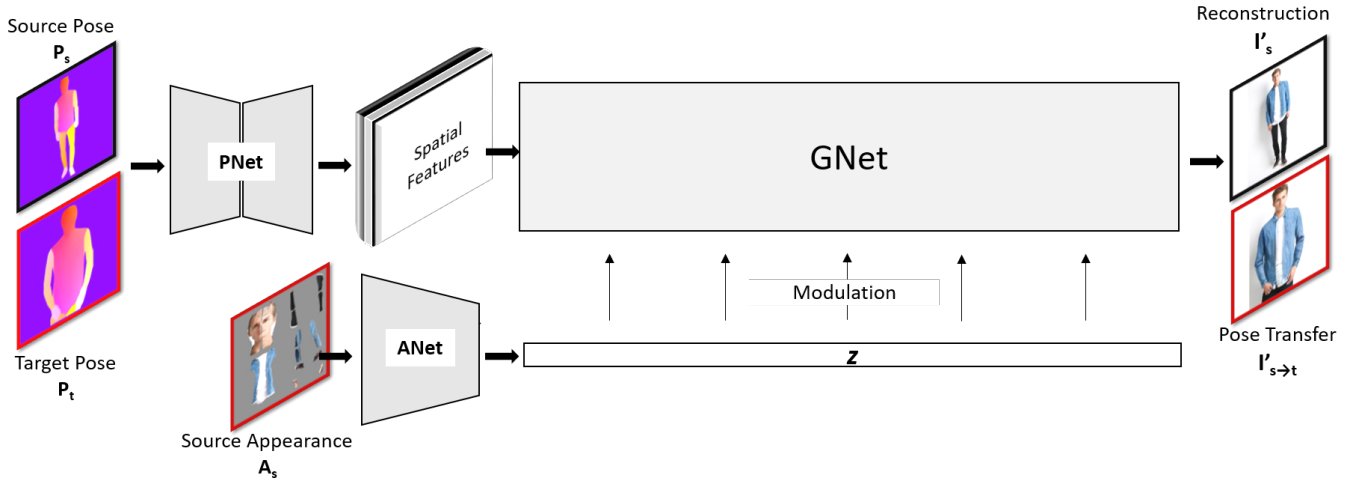


Fig. 4. **Overview of StylePoseGAN:** Given an image I of a person, we extract the pose P and appearance A using DensePose [Gueler et al. 2018]. We then encode the pose and appearance to encodings E and z such that E is a tensor and z is a vector. We finally condition a high-fidelity style-based generator with the extracted pose and appearance to reconstruct back I . The pose and appearance are further disentangled by training with image pairs (I_s, I_t) of the same person with a different pose where we use the appearance of source A_s and the pose of the target P_t to reconstruct I_t . The entire pipeline is trained end-to-end in a fully supervised manner with image reconstruction loss and adversarial loss.

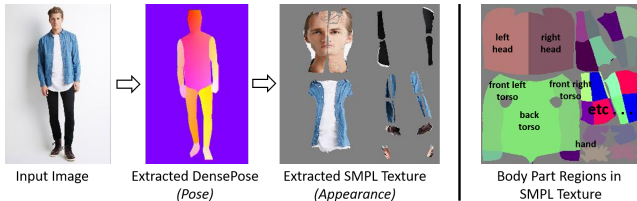


Fig. 5. **Pose and Appearance Extraction.** We use partial texture map of the SMPL mesh as the appearance A and DensePose to represent the pose P of the human. The partial texture image A is divided into 24 part-specific regions p_i (e.g., left head, right head, upper left arm, etc.) as shown on the right. We can provide part-specific conditioning by changing A in the corresponding regions.

Zisserman 2014] applied on I_{gen} and I_{gt} :

$$L_{VGG} = \sum \frac{1}{N^j} |p^j(I_{gen}) - p^j(I_{gt})|, \quad (5)$$

where p^j is the activation and N^j the number of elements of the j -th layer in the VGG network pre-trained on ImageNet.

- **Face Identity Loss.** We use a pre-trained Face Identity Network to enforce similarity of the facial identity between I_{gen} and I_{gt} :

$$L_{face} = |N_{face}(I_{gen}) - N_{face}(I_{gt})|, \quad (6)$$

where N_{face} is the pre-trained SphereFaceNet [Liu et al. 2017b].

- **Adversarial Loss.** We use an adversarial loss L_{GAN} with a discriminator D of the identical architecture as in StyleGAN2 [Karras et al. 2020]. Please refer to StyleGAN2 for further details.

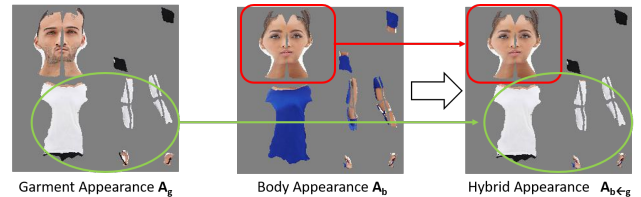


Fig. 6. **Hybrid appearance for garment transfer.** Given the appearance images of the body A_b and garments A_g , we construct a hybrid appearance image $A_{b \leftarrow g}$ with the garment specific regions in A_g and body-specific regions in A_b .

In addition, we use *Patch Discriminator Loss* L_{patch} with a patch co-occurrence discriminator $DPatch$. $DPatch$ is trained such that the patches in I_{gen} can not be distinguished from patches in I_{gt} . A similar idea is used by [Park et al. 2020b] in an unsupervised setting. Please refer to [Park et al. 2020b] for the architecture of $DPatch$.

The final objective \mathcal{L}_{total} is minimised w. r. t. the parameters of $PNet$, $ANet$ and $GNet$, while maximised w. r. t. D and $DPatch$.

3.6 Inference

Once trained, our single trained model can be used for pose transfer, garment and attribute transfer, and interpolation in the learned manifold of appearance. In summary, we can control the pose encoding E and the appearance encoding z independently to accomplish a wide range of tasks.

3.6.1 Pose Transfer. For pose transfer, our method takes a source appearance A_s (that is extracted from a human image), and a target DensePose P_t as input. The re-rendered image of the source person

in the target pose is then obtained as

$$I_{s \rightarrow t} = GNet(PNet(P_t), ANet(A_s)). \quad (7)$$

3.6.2 Garments and Parts Transfer. Once trained for pose transfer, our model can be used for garment transfer without any modification. Given a source body image I_b (with appearance A_b) and a target garment image I_g (with appearance A_g), the aim is to reconstruct the person in I_b with the garments in I_g as $I_{b \leftarrow g}$. To achieve this task, we construct a hybrid appearance image $A_{b \leftarrow g}$ with the garment specific regions in A_g and body-specific regions in A_b , see Fig. 6. The generated image with the swapped garments is then $I_{b \leftarrow g} = GNet(PNet(P_b), ANet(A_{b \leftarrow g}))$. Here $GNet$, $PNet$ and $ANet$ are the trained models for the task of pose transfer.

4 EXPERIMENTAL RESULTS

4.1 Experimental Setup

We use the *In-shop Clothes Retrieval* benchmark of DeepFashion dataset [Liu et al. 2016] for our main experiments. The dataset comprises around 52k high-resolution images of fashion models with 13k different clothing items in different poses. We use the training and testing splits provided by [Siarohin et al. 2019]. To filter non-human images, we discard all the images where we could not compute DensePose, resulting in 38k training images and 3k testing images. We train our system with the resulting training split and use the testing split for conditioning poses. We also show the qualitative results of our method on Fashion dataset [Zablotskaia et al. 2019] that has 500 training and 100 test videos, each containing roughly 350 frames.

We train our model for the task of pose transfer with paired data, as described in Sec. 3.5. In our experiments, texture resolution $H_a \times W_a$ is chosen to be 256×256 , while the output resolution $H \times W$ is chosen to be 256×256 and 512×512 depending on compared methods. The loss weights (Sec. 3.5) are set empirically to $\lambda_{L1} = 1$, $\lambda_{VGG} = 1$, $\lambda_{face} = 1$, $\lambda_{GAN} = 1$, $\lambda_{patch} = 1$. For training, we use ADAM optimiser [Kingma and Ba 2015] with an initial learning rate of 0.002, $\beta_1 = 0.0$ and $\beta_2 = 0.99$. After the convergence of the training, we use the same trained model for all the tasks, *i.e.*, pose transfer, garment transfer, style interpolation and motion transfer.

4.2 Pose Transfer

We perform the experiment of pose transfer using the DeepFashion dataset. Given a human image and a target pose, we re-render the human in the target pose as described in Sec. 3.6.1. Our qualitative results are shown in Figs. 7 and 8.

4.2.1 Comparison with State of the Art. We compare our results with seven state-of-the-art methods: Coordinate Based Inpainting (CBI) [Grigor’ev et al. 2019], Deformable GAN (DSC) [Siarohin et al. 2019], Variational U-Net (VUNet) [Esser et al. 2018], Dense Pose Transfer (DPT) [Neverova et al. 2018], Neural Human Re-Rendering (NHRR) [Sarkar et al. 2020], and ADGAN [Men et al. 2020] at the resolution 256×256 and show the qualitative results in Fig. 7. We train and evaluate our model with the training-testing split provided by Deformable GAN [Siarohin et al. 2019]. This split is also used by all the aforementioned pose transfer methods with the exception of ADGAN [Men et al. 2020]. Training the official implementation

Table 1. Comparison with state-of-the-art methods, using various perceptual metrics, Structural Similarity Index (SSIM) [Zhou Wang et al. 2004] and Learned Perceptual Image Patch Similarity (LPIPS) [Zhang et al. 2018]. \uparrow (\downarrow) means higher (lower) is better. Our approach outperforms all tested methods in both metrics. Note that we improve LPIPS compared to the best previous method NHRR [Sarkar et al. 2020] by $\approx 20\%$.

	SSIM \uparrow	LPIPS \downarrow
DPT [Neverova et al. 2018]	0.759	0.206
VUNet [Esser et al. 2018]	0.739	0.202
DSC [Siarohin et al. 2019]	0.750	0.214
CBI [Grigor’ev et al. 2019]	0.766	0.178
NHRR [Sarkar et al. 2020]	0.768	0.164
StylePoseGAN (ours)	0.788	0.133
GT	1.0	0.0

of ADGAN with our training split did not converge. Therefore, we provide here the results from their trained model in spite of the significant overlap of the testing pairs in their training.

It can be seen that our results show higher realism and better preserve the identity and garment details compared to the other methods. We observe that StylePoseGAN also faithfully reconstructs *high-frequency details*, such as textures and patterns in the garments, which was not captured by any of the competing methods.

We next perform a quantitative evaluation with a subset of the entire testing pairs – 176 testing pairs that are used in the exiting works [Grigor’ev et al. 2019; Sarkar et al. 2020]. The following two metrics were used for comparison:

- *Structural Similarity Index (SSIM)* [Zhou Wang et al. 2004]. SSIM has been widely used in the existing literature for the problem of pose transfer. However, this metric often does not reflect human perception. It is observed that smooth and blurry images tend to have better SSIM than sharper images [Neverova et al. 2018; Zhang et al. 2018].
- *Learned Perceptual Image Patch Similarity (LPIPS)* [Zhang et al. 2018]. LPIPS captures human judgment better than existing hand-designed metrics, making it the most popular and important metric to evaluate generated images. The quantitative results are shown in Table 1. We significantly outperform the existing methods on both metrics. In terms of LPIPS, we observe an improvement of **19%** (from 0.164 to 0.133) over the *previous best result* (NHRR).

4.2.2 User Study. We conduct a user study to assess the visual quality of the pose transfer results by CBI, NHRR and our method. We follow the user study methodology introduced in [Sarkar et al. 2020], *i.e.*, the questions cover a wide variety of source and target poses, and the distribution of males and females roughly reflects the same distribution in the training dataset. Moreover, multiple queries contain artefacts for our method, which make the decisions difficult. For each sample, we ask the following questions:

- (Q1) Which view looks the most like the person in the source image?
- (Q2) Which view looks the most realistic?
- (Q3) Which view preserves fine appearance details (*e.g.*, texture patterns, wrinkles and other elements) better?

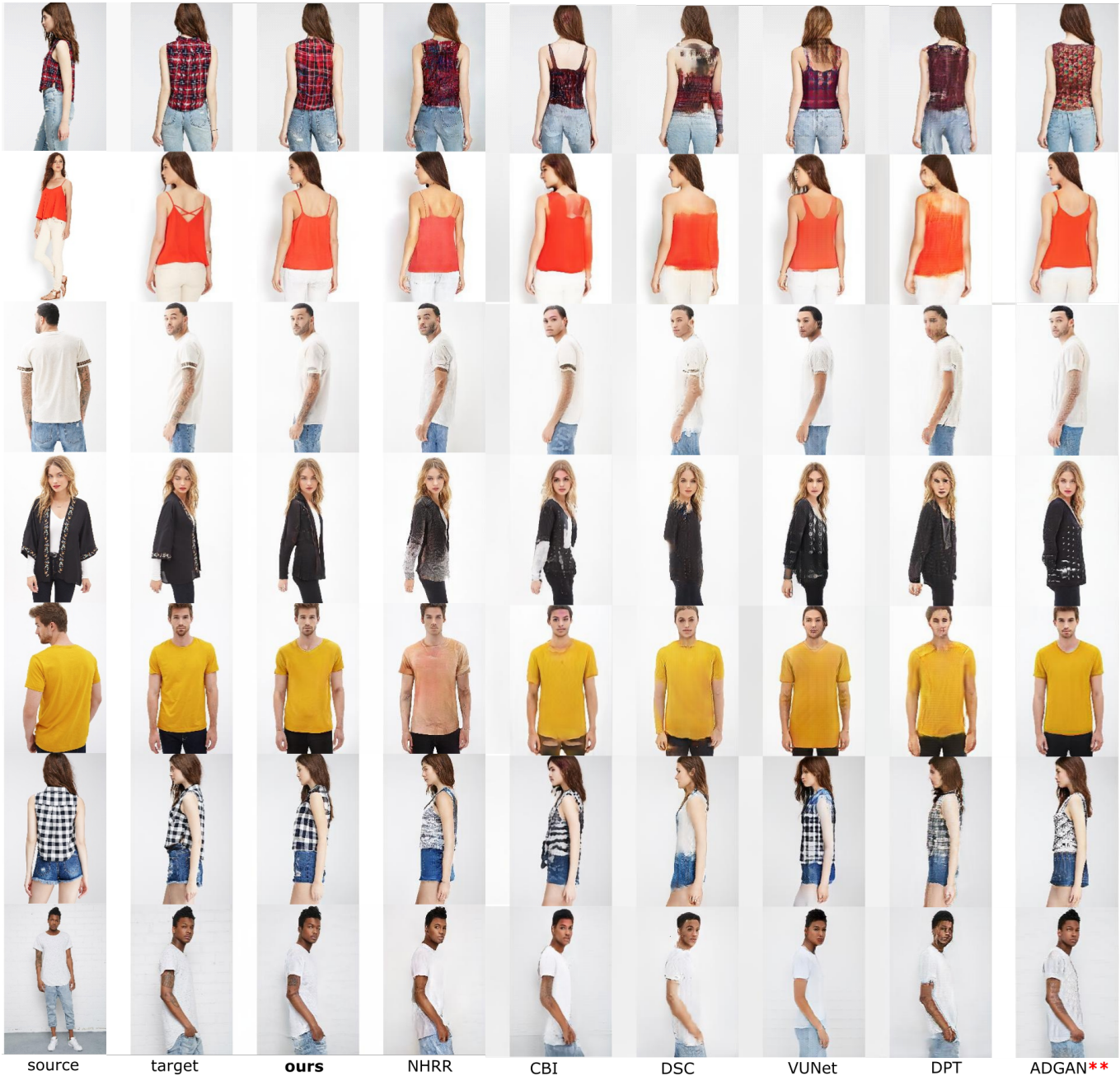
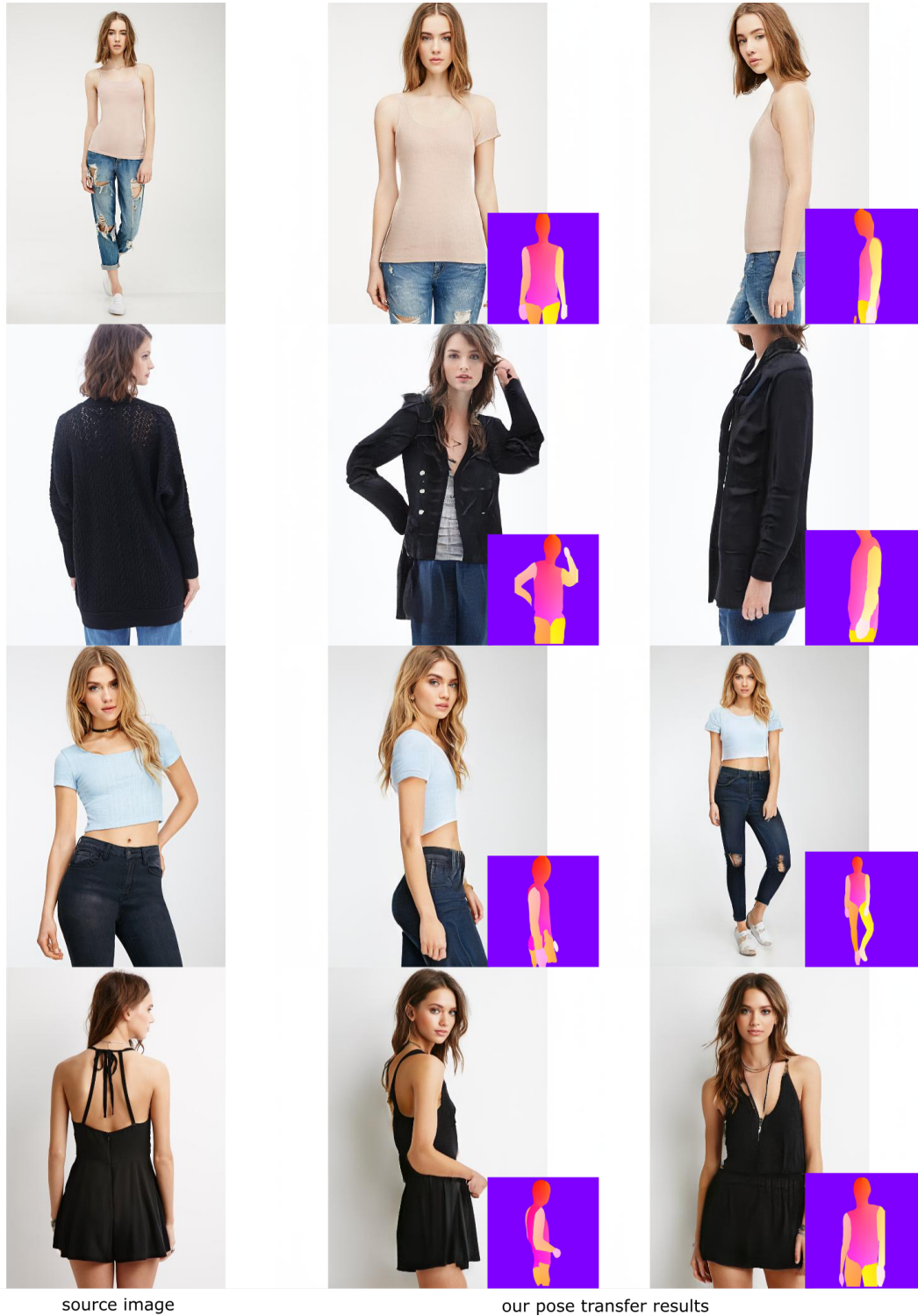


Fig. 7. **Results of our method**, NHRR [Sarkar et al. 2020], CBI [Grigor’ev et al. 2019], DSC [Siarohin et al. 2019], VUNet [Esser et al. 2018], DPT [Neverova et al. 2018], and ADGAN** [Men et al. 2020]. Our approach produces higher-quality renderings and fine-scale details than the competing methods. **The testing pairs were *included* during the training for ADGAN. See Sec. 4.2.1 for more details.

We prepare 46 questions asked in a web-browser user interface in a randomised order. Each question contains a real source image of a person and their pose transfer results (by CBI, NHRR and our method) in randomised order.

27 anonymous respondents have submitted their answers, and the results are summarised in Table 2. Our method ranks first and

is preferred in all three question types by a significant margin compared to CBI and NHRR. CBI is preferred twice out of 144 cases, *i.e.*, once in Q1 (“person similarity”) and once in Q3 (“fine details”), see Fig. 9 for the corresponding image sets. Note that even if CBI was selected two times, the remaining two questions to the same set of images were decided in favour of our method (*e.g.*, CBI preserved



source image

our pose transfer results

Fig. 8. **High-resolution results (512 × 512) of our method for pose transfer.** The conditioning pose is shown on the bottom right for each generated image.



Fig. 9. Two image sets, on which CBI was preferred over other methods, *i.e.*, in Q1 (“person similarity”, top row) and Q3 (“fine details”, bottom row).

Table 2. The summary of the user study.

	CBI	StylePoseGAN (ours)
Q1 (“person similarity”)	2.2%	97.8%
Q2 (“overall realism”)	0%	100%
Q3 (“fine details”)	2.2%	97.8%

the identity best, and, at the same time, StylePoseGAN produces the most realistic rendering with fine details preserved best). According to the final binary per-question rankings, NHRR is not included in Table 2, however, in many cases, it was close to the most frequently voted method (*i.e.*, either CBI or ours). All in all, the user study shows that StylePoseGAN lifts state of the art in pose transfer on a new qualitative level.

4.3 Ablation Study

We perform the following ablation study to see the usefulness of different components. The qualitative results are shown in Fig. 10.

4.3.1 Architecture. The spatial structure P can be directly fed into the generator instead of encoding it through a separate encoder $PNet$. However, the StyleGAN2-like generator takes an input of small spatial dimensions; resizing the pose to such small dimensions (16×16 for the output resolution of 256×256) removes all the meaningful structure information. We, therefore, change $GNet$ with two upsample residual blocks (instead of four in our original design) to take the pose P as input, and completely drop $PNet$ – for the ablation experiment **No-PEncoder**. Because of the large memory requirements by the generator, this baseline takes longer to train. However, after convergence, it performs well and generates high-quality images. In comparison to our full method, *No-PEncoder* takes four times longer to train, and is more unstable with bad input poses as shown in Fig. 10.

Note that style-based generative models can be extended to their conditional version where the conditioning variable is mapped to its style input W (Fig. 3) while keeping the rest of the architecture same, *i.e.*, the spatial tensor S_{input} is a learned constant. However,

we could not bring such network to convergence (with the same generator architecture $GNet$) in our supervised settings. Both of the designs—*i.e.*, mapping of the concatenated pose P and appearance A by an $ANet$ like encoder, and mapping of pose and appearance through separate convolution network followed by fully connected network—did not work. We hypothesise the reasons to be (a) the challenging nature of human images (in comparison to faces) where it is difficult for the mapping network to learn both the appearance and pose together in a single vector, (b) smaller size of our generator in comparison with the StyleGAN which makes it more difficult to learn in these challenging settings and (c) difficulty for a StyleGAN based generators to be extended to the pure conditional scenario. The later case can be mitigated by injecting noise to compromise the supervision errors. However, we did not conduct more exhaustive experiments in this direction, as our primary focus of this work is the spatial condition for style-based generators.

4.3.2 Losses. To see the usefulness of the different loss terms, we perform the experiment **w/o VGG+Face** and **w/o patch concurrency** by removing VGG and face losses, and patch co-occurrence. We see with both qualitative and quantitative results that VGG and face identity losses are crucial for the final results.

4.3.3 Training strategy. We often do not have a training dataset containing images of the same person with multiple poses. To address the issue, we propose the ablation experiment **No-Pairs** where we do not use source-target pairs for the training. Given an image I_s , this design reconstructs back I_s by its own appearance A_s and pose $I'_s = GNet(PNet(P_s), ANet(A_s))$. In addition, we use a random pose from the training set P_t , and use it to reconstruct $I_{s \rightarrow t} = GNet(PNet(P_t), ANet(A_s))$. However, we do not apply any reconstruction loss on $I_{s \rightarrow t}$ because of unavailability of I_t during the training. Instead, we apply patch co-occurrence loss L_{patch} between $I_{s \rightarrow t}$ and I_s . Therefore, the loss objective of Eq. (2) is modified to

$$\mathcal{L}_{total} = \mathcal{L}(I'_s, I_s) + \lambda_{patch} L_{patch}(I'_{s \rightarrow t}, I_t). \quad (8)$$

This experiment accounts for the unsupervised version of our method. We also perform an experiment with the exact setting but with no additional patch co-occurrence loss. A similar method is proposed in swapping autoencoder [Park et al. 2020b]. In contrast to Park et al., this experiment explicitly uses normalised pose and normalised appearance as input which enables better control of the conditioning pose and appearance. This experiment also provides us with the model for garment transfer and has all the advantages of our full method.

The usefulness of the co-occurrence loss can be seen in this unpaired scenario. As observed in Fig. 10, **No-Pairs** with co-occurrence loss performs well. However, it lacks texture details and adds spurious patterns when the poses are too different. *No-pairs* without co-occurrence loss do not preserve appearance. The paired training in our full method version forces the generator to account for the missing texture in highly occluded areas.

4.4 Motion Transfer

Our method can be applied to each frame of a driving video to perform motion transfer. To this end, we keep the image of the source person fixed and use the pose from the actor of the driving

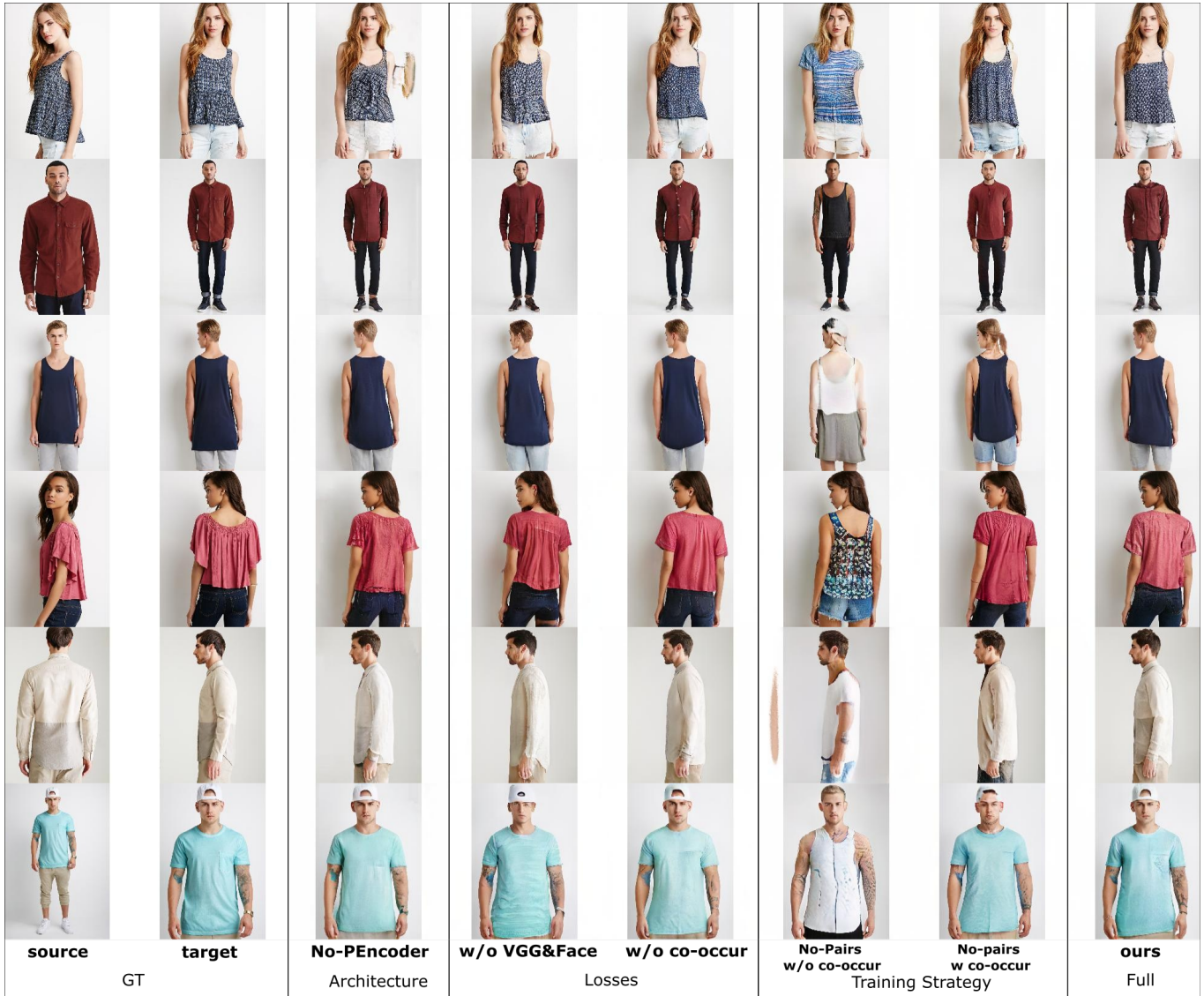


Fig. 10. **Results of our ablation study.** Here, *No-PENcoder* does not use pose encoder, but a generator requiring more memory; *w/o VGG&Face* and *w/o co-occur* do not use VGG/Face and co-occurrence loss, respectively; *No-Pairs* baselines do not use paired training. We observe that our full method performs better than the baselines in almost all cases. The importance of co-occurrence loss during unpaired training is discussed in Sec. 4.3.

video in our system to create image animation. Note that we do not exploit any temporal context, and we create the video frame by frame. We show our result on Fashion Dataset [Zablotskaia et al. 2019] in Fig. 12 and our supplementary video. We observe that our method does not show the shower-curtain effect that is typically present in translation-network-based generators (such as Pix2Pix). Even with the errors and inconsistencies in DensePose on the testing frames, our method keeps the fine wrinkle patterns consistent and provides pose-dependent appearance changes. Note that these wrinkle patterns are learned implicitly by our method through the training data.

4.5 Garment and Part Transfer

As explained in Sec. 3.6.2, our part-based encoding enables our model to perform garment transfer without any further training, *i.e.*, no explicit dataset of garments are needed for our garment transfer functionality. The results are shown in Fig. 13. We observe that StylePoseGAN faithfully reconstructs the garments and body details, and seamlessly generates coherent human images with swapped garments.

The same idea can be used to transfer any other body parts. To this end, we show an example of *head-swap* in Fig. 14. Here we use the hybrid appearance *A* that contains the partial texture of body from one image and head from another image, and the pose from



Fig. 11. **Latent space interpolation.** We can interpolate between two appearance vectors to generate coherently dressed humans with the properties of both target appearances.



Fig. 12. **Motion transfer from a single image.** StylePoseGAN can produce motion animations from a single image from the target sequence. Here, we generate the frames with the pose from *target motion* and appearance from *Source Image*. Please see the accompanying video for the visualisation of pose-dependent appearance changes.

the body image to create the head swap effect. Note that the identity is well preserved even though some conditioning head images are side views.

4.6 Style Interpolation

We find that our latent space is smooth. Interpolating appearance features z_{inter} according to

$$z_{inter} = z_1 t + z_2 (1 - t), \quad t \in [0, 1], \quad (9)$$

where z_1, z_2 are the appearance encodings of two human images, results in images of coherently dressed humans with the properties of both images. Examples are shown in Fig. 11.

5 DISCUSSION

Limitations/Failure Cases. Because we encode the appearance by fully connected layers to a single vector, the spatial semantics in the appearance is destroyed. Therefore, our method has difficulty in reconstructing highly entangled spatial features such as images



Fig. 13. **Our garment transfer results.** The images are generated with the bodies in the row *source body* and garments in the column *target clothes*. Best viewed with zoom.

or text in the clothes (see Figs. 15 and 16). Even in those cases, our method performs better than translation-network-based methods such as NHRR because of the powerful nature of our generator.

6 CONCLUSION

We presented StylePoseGAN, *i.e.*, a new method for synthesising photo-realistic novel views of humans from a single monocular image allowing for explicit control over the pose and appearance without the need for sophisticated 3D modelling. StylePoseGAN significantly outperforms the current state of the art in the perceptual metrics and achieves a high level of realism of the synthesised images in our experiments. The quantitative results are confirmed by a comprehensive user study, in which our results are preferred over competing methods in 142 cases out of 144. We conclude that this is due to improved support of fine texture details of the human appearance such as facial features, textures and shading. The ablation study has confirmed that all design choices are necessary for

the best photo-realistic results. We thus believe that our method, which often produces deceptively realistic renderings, is an important step towards unconstrained novel view rendering of scenes with humans, opening up multiple avenues for future research.

REFERENCES

- Kfir Aberman, Mingyi Shi, Jing Liao, Dani Lischinski, Baoquan Chen, and Daniel Cohen-Or. 2019. Deep Video-Based Performance Cloning. *Computer Graphics Forum* 38, 2 (2019), 219–233.
- Thiemo Alldieck, Gerard Pons-Moll, Christian Theobalt, and Marcus Magnor. 2019. Tex2Shape: Detailed Full Human Body Geometry from a Single Image. In *International Conference on Computer Vision (ICCV)*.
- Aayush Bansal, Shugao Ma, Deva Ramanan, and Yaser Sheikh. 2018. Recycle-GAN: Un-supervised Video Retargeting. In *European Conference on Computer Vision (ECCV)*.
- Andrew Brock, Jeff Donahue, and Karen Simonyan. 2018. Large Scale GAN Training for High Fidelity Natural Image Synthesis. *CoRR* abs/1809.11096 (2018). arXiv:1809.11096 <http://arxiv.org/abs/1809.11096>
- Dan Casas, Marco Volino, John Collomosse, and Adrian Hilton. 2014. 4D Video Textures for Interactive Character Appearance. *Comput. Graph. Forum* 33, 2 (2014), 371–380.
- Caroline Chan, Shiry Ginosar, Tinghui Zhou, and Alexei A Efros. 2019. Everybody Dance Now. In *International Conference on Computer Vision (ICCV)*.



Fig. 14. **Our results of head-swap.** The conditioning image of the head is shown on the bottom for each generated image.



Fig. 15. **Failure cases.** (Left) Encoding the appearance with a vector makes our method difficult to reconstruct highly entangled spatial features such as text. (Right) Bad conditioning DensePose image during the test time deteriorates the output. Also, see Fig. 16 for challenging cases.

Yunjeong Choi, Minje Choi, Munyoung Kim, Jung-Woo Ha, Sunghun Kim, and Jaegul Choo. 2018. StarGAN: Unified Generative Adversarial Networks for Multi-Domain Image-to-Image Translation. In *Computer Vision and Pattern Recognition (CVPR)*.

Patrick Esser, Ekaterina Sutter, and Björn Ommer. 2018. A variational u-net for conditional appearance and shape generation. In *Computer Vision and Pattern Recognition (CVPR)*. 8857–8866.

Guy Gafni, Justus Thies, Michael Zollhöfer, and Matthias Nießner. 2020. Dynamic Neural Radiance Fields for Monocular 4D Facial Avatar Reconstruction. <https://arxiv.org/abs/2012.03065> (2020).

Ian Goodfellow, Jean Pouget-Abadie, Mehdi Mirza, Bing Xu, David Warde-Farley, Sherjil Ozair, Aaron Courville, and Yoshua Bengio. 2014. Generative Adversarial Nets. In *Advances in Neural Information Processing Systems (NeurIPS)*. 2672–2680.

Artur Grigorev, Artem Sevastopolsky, Alexander Vakhitov, and Victor Lempitsky. 2019. Coordinate-Based Texture Inpainting for Pose-Guided Human Image Generation. *Computer Vision and Pattern Recognition (CVPR)* (2019), 12127–12136.

Rieza Alp Gueler, Natalia Neverova, and Iasonas Kokkinos. 2018. DensePose: Dense Human Pose Estimation In The Wild. In *Computer Vision and Pattern Recognition (CVPR)*.

Phillip Isola, Jun-Yan Zhu, Tinghui Zhou, and Alexei A Efros. 2017. Image-to-Image Translation with Conditional Adversarial Networks. In *Conference on Computer Vision and Pattern Recognition (CVPR)*.

Justin Johnson, Alexandre Alahi, and Li Fei-Fei. 2016. Perceptual losses for real-time style transfer and super-resolution. In *European Conference on Computer Vision (ECCV)*. 694–711.

Moritz Kappel, Vladislav Golyanik, Mohamed Elgharib, Jann-Ole Henningson, Hans-Peter Seidel, Susana Castillo, Christian Theobalt, and Marcus Magnor. 2020. High-Fidelity Neural Human Motion Transfer from Monocular Video. arXiv:2012.10974 [cs.CV]

Tero Karras, Timo Aila, Samuli Laine, and Jaakko Lehtinen. 2018. Progressive Growing of GANs for Improved Quality, Stability, and Variation. In *International Conference on Learning Representations (ICLR)*.

Tero Karras, Samuli Laine, and Timo Aila. 2019. A style-based generator architecture for generative adversarial networks. In *Computer Vision and Pattern Recognition (CVPR)*. 4401–4410.

Tero Karras, Samuli Laine, Miika Aittala, Janne Hellsten, Jaakko Lehtinen, and Timo Aila. 2020. Analyzing and Improving the Image Quality of StyleGAN. In *Computer Vision and Pattern Recognition (CVPR)*.

Hyeonwoo Kim, Pablo Garrido, Ayush Tewari, Weipeng Xu, Justus Thies, Matthias Nießner, Patrick Pérez, Christian Richardt, Michael Zollhöfer, and Christian Theobalt. 2018. Deep Video Portraits. *ACM Transactions on Graphics (TOG)* 37 (2018).

Diederick P. Kingma and Jimmy Ba. 2015. Adam: A method for stochastic optimization. In *International Conference on Learning Representations (ICLR)*.

Bernhard Kratzwald, Zhiwu Huang, Danda Pani Paudel, and Luc Van Gool. 2017. Towards an Understanding of Our World by GANing Videos in the Wild. (2017). <https://arxiv.org/abs/1711.11453> arXiv:1711.11453.

Verica Lazova, Eldar Insafutdinov, and Gerard Pons-Moll. 2019. 360-Degree Textures of People in Clothing from a Single Image. *International Conference on 3D Vision (3DV)* (2019), 643–653.

Kathleen M Lewis, Srivatsan Varadharajan, and Ira Kemelmacher-Shlizerman. 2021. VOGUE: Try-On by StyleGAN Interpolation Optimization. *arXiv preprint arXiv:2101.02285* (2021).

Zhengqi Li, Simon Niklaus, Noah Snavely, and Oliver Wang. 2020. Neural Scene Flow Fields for Space-Time View Synthesis of Dynamic Scenes. <https://arxiv.org/abs/2011.13084> (2020).

Lingjie Liu, Jiatao Gu, Kyaw Zaw Lin, Tat-Seng Chua, and Christian Theobalt. 2020a. Neural sparse voxel fields. In *Advances in Neural Information Processing Systems (NeurIPS)*, Vol. 33.

Lingjie Liu, Weipeng Xu, Marc Habermann, Michael Zollhöfer, Florian Bernard, Hyeonwoo Kim, Wenping Wang, and Christian Theobalt. 2020b. Neural Human Video Rendering by Learning Dynamic Textures and Rendering-to-Video Translation. *IEEE*



Fig. 16. **Highly challenging cases.** Even though our method struggles under extreme occlusions, target poses and textures, it synthesises more plausible images than the compared methods.

Transactions on Visualization and Computer Graphics PP (05 2020).

Lingjie Liu, Weipeng Xu, Michael Zollhoefer, Hyeonwoo Kim, Florian Bernard, Marc Habermann, Wenping Wang, and Christian Theobalt. 2019. Neural Rendering and Reenactment of Human Actor Videos. *ACM Transactions on Graphics (TOG)* (2019).

Ming-Yu Liu, Thomas Breuel, and Jan Kautz. 2017a. Unsupervised Image-to-Image Translation Networks. In *International Conference on Neural Information Processing Systems (NeurIPS)*. 700–708.

Weiyang Liu, Yandong Wen, Zhiding Yu, Ming Li, Bhiksha Raj, and Le Song. 2017b. SpheroFace: Deep hypersphere embedding for face recognition. In *Computer Vision and Pattern Recognition (CVPR)*. 212–220.

Z. Liu, P. Luo, S. Qiu, X. Wang, and X. Tang. 2016. DeepFashion: Powering Robust Clothes Recognition and Retrieval with Rich Annotations. In *Computer Vision and Pattern Recognition (CVPR)*. 1096–1104.

Stephen Lombardi, Tomas Simon, Jason Saragih, Gabriel Schwartz, Andreas Lehrmann, and Yaser Sheikh. 2019. Neural Volumes: Learning Dynamic Renderable Volumes from Images. *ACM Trans. Graph. (SIGGRAPH)* 38, 4 (2019).

Matthew Loper, Naureen Mahmood, Javier Romero, Gerard Pons-Moll, and Michael J. Black. 2015. SMPL: A Skinned Multi-Person Linear Model. *ACM Trans. Graphics (Proc. SIGGRAPH Asia)* 34, 6 (2015), 248:1–248:16.

Liqian Ma, Xu Jia, Qianru Sun, Bernt Schiele, Tinne Tuytelaars, and Luc Van Gool. 2017. Pose guided person image generation. In *Advances in Neural Information Processing Systems (NeurIPS)*. 405–415.

Liqian Ma, Qianru Sun, Stamatios Georgoulis, Luc van Gool, Bernt Schiele, and Mario Fritz. 2018. Disentangled Person Image Generation. *Computer Vision and Pattern Recognition (CVPR)* (2018).

Yifang Men, Yiming Mao, Yuning Jiang, Wei-Ying Ma, and Zhouhui Lian. 2020. Controllable Person Image Synthesis with Attribute-Decomposed GAN. In *Computer Vision and Pattern Recognition (CVPR)*.

Moustafa Meshry, Dan B. Goldman, Sameh Khamis, Hugues Hoppe, Rohit Pandey, Noah Snavely, and Ricardo Martin-Brualla. 2019. Neural Rerendering in the Wild. In *Computer Vision and Pattern Recognition (CVPR)*.

Ben Mildenhall, Pratul P. Srinivasan, Matthew Tancik, Jonathan T. Barron, Ravi Ramamoorthi, and Ren Ng. 2020. NeRF: Representing scenes as neural radiance fields for view synthesis. In *European Conference on Computer Vision (ECCV)*.

Mehdi Mirza and Simon Osindero. 2014. Conditional Generative Adversarial Nets. *CoRR* abs/1411.1784 (2014). arXiv:1411.1784 [cs.LG]

Takeru Miyato and Masanori Koyama. 2018. cGANs with Projection Discriminator. In *International Conference on Learning Representations (ICLR)*.

Natalia Neverova, Riza Alp Güler, and Iasonas Kokkinos. 2018. Dense Pose Transfer. *European Conference on Computer Vision (ECCV)* (2018).

Augustus Odena, Christopher Olah, and Jonathon Shlens. 2017. Conditional Image Synthesis with Auxiliary Classifier GANs (*Proceedings of Machine Learning Research (PMLR)*). 2642–2651.

Keunhong Park, Utkarsh Sinha, Jonathan T. Barron, Sofien Bouaziz, Dan Goldman, Steven Seitz, and Ricardo Martin-Brualla. 2020a. Deformable Neural Radiance Fields. <https://arxiv.org/abs/2011.12948> (2020).

Taesung Park, Ming-Yu Liu, Ting-Chun Wang, and Jun-Yan Zhu. 2019. Semantic Image Synthesis with Spatially-Adaptive Normalization. In *Computer Vision and Pattern Recognition (CVPR)*.

Taesung Park, Jun-Yan Zhu, Oliver Wang, Jingwan Lu, Eli Shechtman, A. Alexei Efros, and Richard Zhang. 2020b. Swapping Autoencoder for Deep Image Manipulation. In *Advances in Neural Information Processing Systems (NeurIPS)*.

Albert Pumarola, Antonio Agudo, Alberto Sanfeliu, and Francesc Moreno-Noguer. 2018. Unsupervised Person Image Synthesis in Arbitrary Poses. In *Computer Vision and Pattern Recognition (CVPR)*.

Albert Pumarola, Enric Corona, Gerard Pons-Moll, and Francesc Moreno-Noguer. 2020. D-NeRF: Neural Radiance Fields for Dynamic Scenes. <https://arxiv.org/abs/2011.13961> (2020).

Amit Raj, Michael Zollhoefer, Tomas Simon, Jason Saragih, Shunsuke Saito, James Hays, and Stephen Lombardi. 2020. PVA: Pixel-aligned Volumetric Avatars. In *arXiv:2101.02697*.

Kripasindhu Sarkar, Dushyant Mehta, Weipeng Xu, Vladislav Golyanik, and Christian Theobalt. 2020. Neural Re-Rendering of Humans from a Single Image. In *European Conference on Computer Vision (ECCV)*.

Alon Shoshan, Nadav Bhoneker, Igor Kviatkovsky, and Gerard Medioni. 2021. GAN-Control: Explicitly Controllable GANs. arXiv:2101.02477 [cs.CV]

Aliaksandr Siarohin, Stéphane Lathuilière, Enver Sangineto, and Nicu Sebe. 2019. Appearance and Pose-Conditioned Human Image Generation using Deformable GANs. *Transactions on Pattern Analysis and Machine Intelligence (TPAMI)* (2019).

Aliaksandr Siarohin, Enver Sangineto, Stéphane Lathuilière, and Nicu Sebe. 2018. Deformable GANs for Pose-based Human Image Generation. In *Computer Vision and Pattern Recognition (CVPR)*.

Yinghao Xu, Qianqian Wang, Qing Shuai, Hujun Bao, Xiaowei Zhou, Sida Peng, Yuanqing Zhang. 2020. Neural Body: Implicit Neural Representations with Structured Latent Codes for Novel View Synthesis of Dynamic Humans. *arXiv preprint arXiv:2012.15838* (2020).

Karen Simonyan and Andrew Zisserman. 2014. Very deep convolutional networks for large-scale image recognition. *arXiv preprint arXiv:1409.1556* (2014).

Vincent Sitzmann, Justus Thies, Felix Heide, Matthias Nießner, Gordon Wetzstein, and Michael Zollhöfer. 2019a. DeepVoxels: Learning Persistent 3D Feature Embeddings. In *Computer Vision and Pattern Recognition (CVPR)*.

Vincent Sitzmann, Michael Zollhöfer, and Gordon Wetzstein. 2019b. Scene Representation Networks: Continuous 3D-Structure-Aware Neural Scene Representations. In *Advances in Neural Information Processing Systems (NeurIPS)*.

Ayush Tewari, Mohamed Elgharib, Gaurav Bharaj, Florian Bernard, Hans-Peter Seidel, Patrick Pérez, Michael Zöllhofer, and Christian Theobalt. 2020a. StyleRig: Rigging StyleGAN for 3D Control over Portrait Images. In *Computer Vision and Pattern Recognition (CVPR)*.

Ayush Tewari, Mohamed Elgharib, Mallikarjun BR, Florian Bernard, Hans-Peter Seidel, Patrick Pérez, Michael Zöllhofer, and Christian Theobalt. 2020b. PIE: Portrait Image

- Embedding for Semantic Control. *ACM Transactions on Graphics (Proceedings SIGGRAPH Asia)* 39, 6 (2020).
- Justus Thies, Michael Zollhöfer, and Matthias Nießner. 2019. Deferred neural rendering: image synthesis using neural textures. *ACM Transactions on Graphics (TOG)* 38 (2019).
- Edgar Tretschk, Ayush Tewari, Vladislav Golyanik, Michael Zollhöfer, Christoph Lassner, and Christian Theobalt. 2020. Non-Rigid Neural Radiance Fields: Reconstruction and Novel View Synthesis of a Deforming Scene from Monocular Video. <https://arxiv.org/abs/2012.12247> (2020).
- Gül Varol, Javier Romero, Xavier Martin, Naureen Mahmood, Michael J. Black, Ivan Laptev, and Cordelia Schmid. 2017. Learning from Synthetic Humans. In *Computer Vision and Pattern Recognition (CVPR)*.
- Marco Volino, Dan Casas, John Collomosse, and Adrian Hilton. 2014. Optimal Representation of Multiple View Video. In *Proceedings of the British Machine Vision Conference*. BMVA Press.
- Ting-Chun Wang, Ming-Yu Liu, Jun-Yan Zhu, Guilin Liu, Andrew Tao, Jan Kautz, and Bryan Catanzaro. 2018a. Video-to-Video Synthesis. In *Advances in Neural Information Processing Systems (NeurIPS)*.
- Ting-Chun Wang, Ming-Yu Liu, Jun-Yan Zhu, Andrew Tao, Jan Kautz, and Bryan Catanzaro. 2018b. High-Resolution Image Synthesis and Semantic Manipulation with Conditional GANs. In *Computer Vision and Pattern Recognition (CVPR)*.
- Ziyan Wang, Timur Bagautdinov, Stephen Lombardi, Tomas Simon, Jason Saragih, Jessica Hodgins, and Michael Zollhöfer. 2020. Learning Compositional Radiance Fields of Dynamic Human Heads. [arXiv:2012.09955](https://arxiv.org/abs/2012.09955) [cs.CV]
- Wenqi Xian, Jia-Bin Huang, Johannes Kopf, and Changil Kim. 2020. Space-time Neural Irradiance Fields for Free-Viewpoint Video. <https://arxiv.org/abs/2011.12950> (2020).
- Feng Xu, Yebin Liu, Carsten Stoll, James Tompkin, Gaurav Bharaj, Qionghai Dai, Hans-Peter Seidel, Jan Kautz, and Christian Theobalt. 2011. Video-based Characters: Creating New Human Performances from a Multi-view Video Database. In *ACM SIGGRAPH*. 32:1–32:10.
- Zili Yi, Hao Zhang, Ping Tan, and Minglun Gong. 2017. DualGAN: Unsupervised Dual Learning for Image-to-Image Translation. In *International Conference on Computer Vision (ICCV)*. 2868–2876.
- Jae Shin Yoon, Lingjie Liu, Vladislav Golyanik, Kripasindhu Sarkar, Hyun Soo Park, and Christian Theobalt. 2020. Pose-Guided Human Animation from a Single Image in the Wild. [arXiv:2012.03796](https://arxiv.org/abs/2012.03796) [cs.CV]
- Polina Zablotkaia, Aliaksandr Siarohin, Leonid Sigal, and Bo Zhao. 2019. DwNet: Dense warp-based network for pose-guided human video generation. In *British Machine Vision Conference (BMVC)*.
- Han Zhang, Ian Goodfellow, Dimitris Metaxas, and Augustus Odena. 2019. Self-Attention Generative Adversarial Networks (*Proceedings of Machine Learning Research (PMLR)*). 7354–7363.
- Kai Zhang, Gernot Riegler, Noah Snavely, and Vladlen Koltun. 2020. NERF++: Analyzing and Improving Neural Radiance Fields. <https://arxiv.org/abs/2010.07492> (2020).
- Richard Zhang, Phillip Isola, Alexei A Efros, Eli Shechtman, and Oliver Wang. 2018. The Unreasonable Effectiveness of Deep Features as a Perceptual Metric. In *Computer Vision and Pattern Recognition (CVPR)*.
- Zhou Wang, Alan C. Bovik, Hamid R. Sheikh, and Eero P. Simoncelli. 2004. Image quality assessment: from error visibility to structural similarity. *IEEE Transactions on Image Processing* 13, 4 (2004), 600–612.
- Jun-Yan Zhu, Taesung Park, Phillip Isola, and Alexei A. Efros. 2017. Unpaired Image-to-Image Translation using Cycle-Consistent Adversarial Networks. In *International Conference on Computer Vision (ICCV)*.
- Zhen Zhu, Tengting Huang, Baoguang Shi, Miao Yu, Bofei Wang, and Xiang Bai. 2019. Progressive Pose Attention Transfer for Person Image Generation. In *Computer Vision and Pattern Recognition (CVPR)*. 2347–2356.